# Parametric Optimisation Of Spot Welding Of 17-4 Ph Stainless Steels Using The Analytic Hierarchy Process

**Chinmoy Mondal[1], Subhajit Bhattacharya[2] and Santanu Das[3]***
Department of Mechanical Engineering, Kalyani Government Engineering College, Kalyani- 741235.
Email: [1]chinmoy.mpe@gmail.com, [2]sbhattacharya63@gmail.com, [3]sdas.me@gmail.com
*Corresponding author

## ABSTRACT

Resistance spot welding is traditionally employed for joining thin sheet metals. However, flawless resistance spot welding of steels with large amount of alloying elements is a challenge to the welding engineers and scientists. In this work, resistance spot welding is done on 17-4 precipitation hardened stainless steel sheets that are widely applied in aerospace industries. Effect of variation of set weld current and welding time on the weldment is investigated. First, welding time is varied keeping weld current constant, and then, under a constant welding time, weld current is varied. Weld nugget diameter and its form are observed macroscopically, and tensile shear load tests are done to determine the spot strength. Metallographic observation is made to compare the heat affected zone and the weld zone. Details of the experimental conditions and procedure are presented in this paper. The Analytical Hierarchy Process (AHP) is then applied to optimize the process parameters within the experimental domain. The optimal condition to have a quality weld is found at 5 cycles of welding time and 8 kA of set weld current under a load of 4 kN.

**Keywords:** Welding, resistance spot welding, AHP, Analytic Hierarchy Process, parametric optimization

## INTRODUCTION

Resistance spot welding is a process of joining two or more overlapped metal sheets by fusion at discrete spots at the sheet interface. This process was invented in 1877 by E. Thomson and has been extensively used since then in the manufacturing industries for joining metal sheets. Two main industries that widely use this process are automobile industries and aircraft industries [1,2]. Resistance to current flow through the metal sheets generates heat, and temperature rise at the sheet interface is allowed till the plastic point of metal is reached. Then metal interface begins to fuse and nugget is formed. Current is switched off, and the nugget is allowed to cool down slowly to solidify under pressure. This process is completed within a specified cycle time.

The strength of spot-weld depends on several factors like structure and property of base metals, characteristics and configuration of the weld, size and geometry of the specimen, mode of loading, test conditions, etc. Several researchers [3,4] have examined the influence of these factors to predict failure of spot-welds, and thus, improve the reliability of the weld. Vural et al. [5,6] have carried out some experiments on the resistance spot weldability of galvanized interstitial free steel sheet with austenitic stainless steel sheet. They have found that with the increase in current, the nugget diameter increases up to certain limit, and after that it decreases. They have also found that with the increase of the nugget diameter, tensile-shear strength of the spot welded joint increases, and nugget formation is more active in stainless steel sheets having higher electrical resistance. Kahraman [7] has shown that increasing welding time and electrode force increases the tensile shearing strength, and he has observed that the joints obtained under the argon atmosphere have better tensile-shearing strength. Aslanlar et al. [8] has investigated the effect of weld current and welding time on tensile shear strength of automotive sheet in resistance spot welding. Mukhopadhyay et al. [9] has carried out some studies to investigate the effects of nugget diameter, mode of loading and alloy chemistry on the strength of spot-welds in thin sheets of interstitial free steels. A number of other researchers [10-27] have conducted tests to characterize resistance spot welding to suite different similar and dissimilar metals and alloys. Different algorithms have also been used to optimize welding process parameters, such as artificial neural networks (NN) [25], the analytical hierarchy process (AHP) [28,29], grey relational analysis along with Taguchi method [30], etc.

The aim of the present work is to optimize welding parameters for spot welding of 17-4 precipitation hardened (PH) stainless steel, which is to apply to in aircraft components, to obtain sound weld within the experimental domain.

## EXPERIMENTAL DETAILS

For this study, specimens used are of 17–4 PH stainless steel, typically with 17% Cr, 4% Ni, 1% Mn, 1% Si and 4% Cu, cut in the size of 100 mm x 25 mm x 0.6 mm. Suitable tabs of 25 mm x 25 mm are provided at the end of two specimens for the tensile shear test. Faying surfaces of specimens are cleaned with acetone to eliminate surface contamination before resistance spot welding. The test is carried out using current and time controlled electric resistance spot welding machine. This machine is equipped with a variable pneumatic pressure system. Welding, squeezing and holding times are adjusted. The resistance spot welding machine is of Sonder Technologies Ltd. make with Bosch PS200 welding controller.

Parameters considered for the experiment are weld current and welding time with constant electrode force. For each parameter set, four specimens are prepared. At each parameter group, three welded specimens are used to make the tensile shear test specimen while the remaining one is used for macrostructure examination. The parameter varied during experiment set I is welding time, expressed in terms of cycles (1 cycle= 1/50 second), with a constant weld current of 2.5 kA (Table 1). In experiment set II, weld current is varied from 3 to 9 kA while welding time is kept constant at 5 cycles (Table 2).

**Table 1:** Specimens for varying welding time while keeping weld current constant at 2.5 kA

| Specimens | Welding time in cycles |
|---|---|
| 1A, 1B, 1C, 1D | 3 |
| 2A, 2B, 2C, 2D | 4 |
| 3A, 3B, 3C, 3D | 5 |
| 4A, 4B, 4C, 4D | 6 |
| 5A, 5B, 5C, 5D | 7 |
| 6A, 6B, 6C, 6D | 8 |
| 7A, 7B, 7C, 7D | 9 |

**Table 2 :** Specimens for varying welding current while keeping welding time constant at 5 cycles

| Specimens | Welding current in kA |
|---|---|
| 8A, 8B, 8C, 8D | 3 |
| 9A, 9B, 9C, 9D | 4 |
| 10A, 10B, 10C, 10D | 5 |
| 11A, 11B, 11C, 11D | 6 |
| 12A, 12B, 12C, 12D | 7 |
| 13A, 13B, 13C, 13D | 8 |
| 14A, 14B, 14C, 14D | 9 |

Following standard equation is used for finding the electrode tip diameter to apply to low alloy steels.

$$D = 0.100 + 2t \quad (1)$$

where, 't' is thickness in inch of the metal sheet to weld. In the present case, sheet thickness used is 0.6 mm, and for it, electrode tip diameter is calculated to be 4 mm.

In order to determine tensile shear load bearing capacity of weldment, a Universal Testing Machine of class-1 level (make: Alfred J. Amsler & Co., Switzerland) is used. For carrying out the test, the specimen ends are spot welded with a 25mm x 25 mm sheet, so that proper gripping is provided for the specimen. The built-in dynamometer indicates the load applied with a maximum error of ± 0.5%.

Metallographic examination is carried out to observe the macrostructure of the weld and heat affected zones. For this, samples are prepared by sectioning the weld at the middle in a direction perpendicular to the application of pressure. These samples are subsequently prepared for metallographic examination by grinding using rough and fine emery papers, followed by polishing. They are etched using a solution of 15 ml HCl, 15 ml HNO3 and 70 ml water for 10 minutes, and are examined using metallurgical, and tool makers microscopes.

## RESULTS AND DISCUSSION

Weld quality is determined by the joint strength, weld nugget size, weld penetration, sheet separation, and internal discontinuities. The surface appearance of a spot weld needs be relatively smooth, round or oval in the case of contoured work, and free from surface fusion, electrode deposit, pit, crack and deep electrode indentation [7]. Good surface appearance can be achieved by properly cleaning surfaces of samples before welding and proper selection of process parameters. Overheating between electrodes and workpieces causes surface flashing, pick up of metal on the electrode, and poor surface appearance [11,12]. In the present study, to check the quality of weld, nugget diameter is found from the macrostructure of the spot welded specimens. In order to evaluate the weld quality of joined materials, the strength of weldment is also determined.

Smooth weld surface appearance is almost always obtained in this study. The extent of indentation of electrode present in the welded sample is found acceptable. Good appearance of the weld surface may be attributed to cleaning of samples prior to welding. In some spot welds, high material expulsions are observed, that may be due to overheating between electrodes and workpieces due to high heat input.

**Shear Strength of the Joint**

In the present study, weld joints are subjected to tensile shear test in order to evaluate the weld quality. At each parameter combination, three welded specimens (A, B and C) are made to undergo tensile shear test. Spot strength of specimens made under varying welding time keeping weld current constant at 2.5 kA is measured and shown in Fig.1. The solid line of the plot corresponds to average spot strength, and maximum and minimum values of spot strength, that is, the scatter at each welding time are also depicted in Fig.1. Average value of spot strength does not vary much up to 8 cycles of welding time. However, minimum spot strength is seen at 8 cycles, and then there is a steep hike in it for welding time of 9 cycles.

Heat transfer is a function of time, and the development of the proper nugget size requires a minimum length of time, regardless of weld current. The enhancement in tensile shear load bearing capacity of weldment may be primarily attributed to the enlargement of size of a flawless nugget. Some researchers also have reported that the nugget size of weldment increases with increasing heat input related to either weld current or welding time, so that strength of weldment increases [10]. At higher welding time or current, excessive heat energy input may cause void and crack formation, partially spurt out of molten metal, etc., and hence, may not be adopted. In the present work, beyond 8 cycles of welding time, large rise in spot strength is seen from Fig.1. At a welding time of 9 cycles, nugget diameter is measured to be lesser than that of lower welding time, and load bearing capacity is also less.

Spot strengths of specimens for varying weld current keeping welding time constant (5 cycles) are measured and depicted in Fig. 2 showing average spot strength of three different specimens (specimen A, B and C) welded at each welding parameter combination along with the minimum and maximum values (scatter) at each welding current. From Fig. 2, no clear trend in changes in spot strength with the increase in weld current is observed.

Although spot strength is expected to be dependent on nugget size, and it may increase with increasing heat input related to either weld current or welding time [7], in the present work, no clear trend is observed within the experimental domain considered.

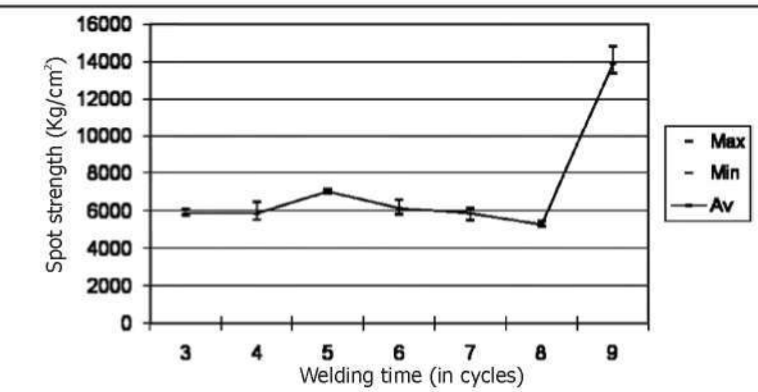


**Fig. 1:** Plot of average spot strength with welding time at 2.5 kA weld current

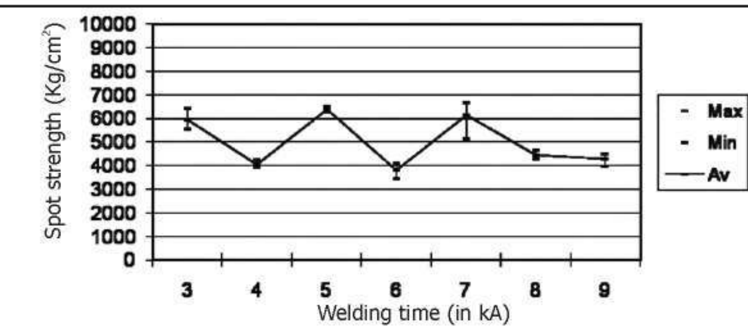


**Fig. 2 :** Plot of average spot strength with weld current keeping welding time constant at 5 cycles

## Nugget Size

The nugget diameter is considered to be an important parameter in determination of spot weld quality [7]. The quality and approximate strength of the weld can be estimated by measuring its diameter and depth of fusion. The diameter or width of the fused zone needs to meet the requirement of appropriate specifications or the design criteria.

Nugget diameter is measured from the macrostructure of the spot welded specimens, and results are shown in Table 3 and Table 4 for varying weld current at constant welding time, and varying welding time at constant weld current respectively. Therefore, an attempt is made to optimize the welding performance relating to nugget diameter and welding parameters.

Nugget size (diameter) for all welding conditions are found to be higher than a minimum requirement [9] of nugget diameter of 3.5–4 times the thickness of the joint materials. Except at a welding time of 9 cycles at weld current of 2.5 kA, when nugget diameter is quite less, other welding conditions show large spot size and acceptable strength.

**Table 3:** Variation of nugget diameter with welding time at a constant weld current of 2.5 kA

| Sl. No. | Welding time (cycles) | Nugget diameter (mm) |
|---|---|---|
| 1 | 3 | 3.386 |
| 2 | 4 | 3.495 |
| 3 | 5 | 3.286 |
| 4 | 6 | 3.5 |
| 5 | 7 | 3.6 |
| 6 | 8 | 3.684 |
| 7 | 9 | 2.191 |

Nugget diameter of spot weld for varying welding current keeping welding current constant at 2.5 kA is measured in first set of experiments; corresponding results are presented in Table 3. It is seen that the nugget diameter increases on the whole with the increase in welding time till a critical value of 3.684 mm at a welding time of 8 cycles. The increase in welding time, that causes enhancement of heat input, in turn, results in an increase in nugget size of the weld up to 8 cycles of welding time. After that, diameter decreases drastically to 2.191 mm at 9 cycles of welding time. At this condition, spilling out of material and void formation inside the nugget (Fig. 1) may have resulted in nugget diameter. This finding is in-line with the work reported earlier [13].

In the second case, when welding time is kept constant at 5 cycles, and weld current is increased in steps of 1 kA from 3 kA to 9 kA, change in weld current does not give a clear trend in change in nugget diameter (Table 4). However, higher nugget diameters more than 4.85 mm are achieved at the weld current of 8-9 kA. Average diameter for 3 kA to 7 kA is seen to be within 3.4 mm and 4.4 mm. After a weld current of 7 kA, increase in current leads to increase in nugget diameter; it may be attributed to the increasing welding current that causes enhancement of heat input. This, in turn, may have resulted in an increase in nugget size of the weld. This observation is also supported by the earlier work of Marashi et al. [10].

Typical structures of the weld nugget obtained under varying weld time are shown in Fig. 3(a-d). Fig. 3(a-c) shows acceptable nugget formation, whereas Fig. 3(d) shows the HAZ having weld defects. Up to a welding time, HAZ (Heat Affected Zone) increases with the increase in welding time, and welding defects are observed at quite high welding time. Good weld nugget is observed at 6 welding cycles at a constant welding current of 2.5 kA. Only 50% of material is melted in this case as optimum is considered at 40%- 60% [13].

**Table 4:** Variation of nugget diameter with weld current at a constant weld time of 5 cycles

| Sl. No. | Weld current (kA) | Nugget diameter (mm) |
|---|---|---|
| 1 | 3 | 3.474 |
| 2 | 4 | 4.292 |
| 3 | 5 | 3.409 |
| 4 | 6 | 4.393 |
| 5 | 7 | 3.772 |
| 6 | 8 | 4.856 |
| 7 | 9 | 4.923 |

Similar structural views are observed under varying weld current as shown in Fig. 4(a-d). In this case, for Fig. 4(a-b), good nugget is obtained; however, Fig. 4(c) shows some white spots, but no voids, and Fig. 4(d) indicates high electrode indentation and noticeable pores inside the weld zone. It is observed that at higher current, nugget area increases expectedly, and at 9 kA, sizeable defects are observed (Fig. 4(d)).

## Application of the Analytical Hierarchy Process for Finding out the Optimum Condition

The Analytic Hierarchy Process (AHP), introduced by Saaty [31], is used in this work to find out the optimum process parameters in resistance spot welding of stainless steel specimens within the experimental domain. The AHP algorithm used in this work has been detailed in the other papers [28,29] of

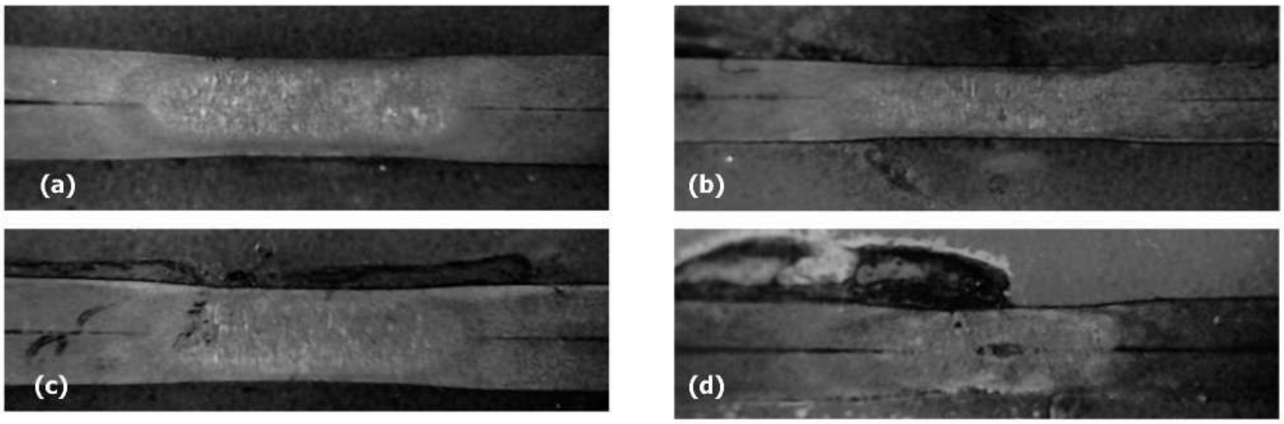


**Fig. 3 :** Macrostructure of nuggets under varying welding time (T) at a constant weld current of 2.5 kA (a) T = 6 cycles, (b) T = 7 cycles, (c) T = 8 cycles, and (d) T = 9 cycles.

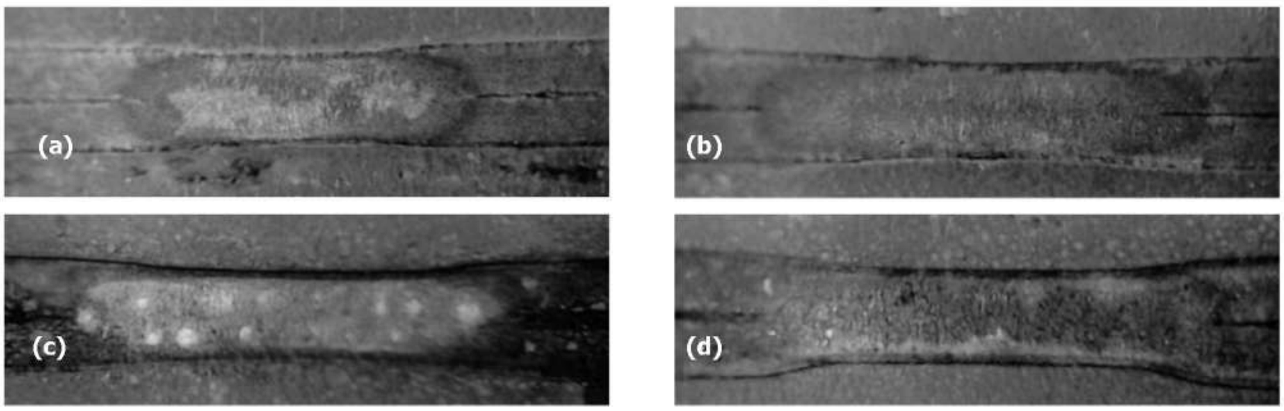


**Fig. 4 :** Macrostructure of nuggets with varying weld current (I) at constant welding time of 5 cycles (a) I = 6 kA, (b) I = 7 kA, (c) I = 8 kA, and (d) I = 9 kA.

the corresponding author. First, the hierarchy structure is constructed (Fig. 5). At the top of the hierarchy is the overall goal, which in this case, is optimization of process parameters. At the middle level of the hierarchy are the criteria. Alternatives come at the bottom most level.

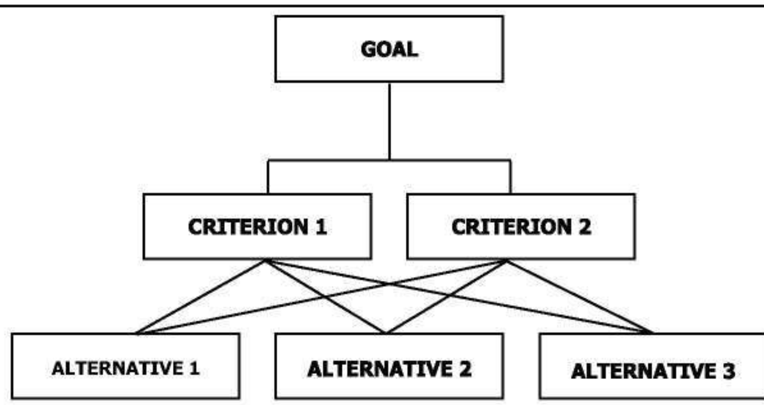


**Fig. 5 :** Hierarchy structure of the AHP Used

The alternatives considered are different combinations of parameters and are listed in first three columns of Table 5. Each combination forms one alternative, and there are 14 such variations forming fourteen alternatives. Three criteria for evaluating the weld quality are chosen, and these are weld spot appearance and penetration (C1), tensile shear strength (C2) and nugget diameter (C3) as listed in Table 6. The criteria matrix to optimize resistance spot welding (RSW) within the experimental domain is shown in Table 7. The weights assigned at each matrix element are chosen following 1, 2, ...., 9 and 1/9, 1/8, ..., ½, 1 ratio scale suggested by Saaty [31].

| **Table 5:** Experimental observations | | | | |
|---|---|---|---|---|
| Alternatives | Weld current (kA) | Welding time (in cycles) | Bending load (in kg) | Nugget diameter (mm) |
| A1 | 2.5 | 3 | 530 | 3.386 |
| A2 | 2.5 | 4 | 563 | 3.495 |
| A3 | 2.5 | 5 | 598 | 3.286 |
| A4 | 2.5 | 6 | 595 | 3.5 |
| A5 | 2.5 | 7 | 598 | 3.6 |
| A6 | 2.5 | 8 | 563 | 3.684 |
| A7 | 2.5 | 9 | 576 | 2.191 |
| A8 | 3 | 5 | 562 | 3.474 |
| A9 | 4 | 5 | 586 | 4.292 |
| A10 | 5 | 5 | 582 | 3.409 |
| A11 | 6 | 5 | 578 | 4.393 |
| A12 | 7 | 5 | 686 | 3.772 |
| A13 | 8 | 5 | 825 | 4.856 |
| A14 | 9 | 5 | 815 | 4.923 |

| **Table 6:** The Criteria | |
|---|---|
| Symbol | Criteria |
| C1 | Weld spot appearance and Penetration |
| C2 | Tensile Shear Strength (Spot Strength) |
| C3 | Nugget Diameter |

| **Table 7:** The Criteria Matrix | | | | |
|---|---|---|---|---|
| To optimize RSW | C1 | C2 | C3 | Local Weight |
| C1 | 1 | 1/6 | 1/4 | 0.086948 |
| C2 | 6 | 1 | 3 | 0.639334 |
| C3 | 4 | 1/3 | 1 | 0.273718 |

The principal eigen value, $\lambda_{max}$ = 3.053678, CR = 0.008343

| **Table 8 :** Alternative matrix with respect to Criteria C1, Penetration and Spot Appearance | | | | | | | | | | | | | | | |
|---|---|---|---|---|---|---|---|---|---|---|---|---|---|---|---|
| C1 | A1 | A2 | A3 | A4 | A5 | A6 | A7 | A8 | A9 | A10 | A11 | A12 | A13 | A14 | Local Weight |
| A1 | 1 | 1 | 1 | 1/4 | ½ | ½ | 1 | 1/2 | 1/2 | 1/2 | 1/4 | 1/2 | 1 | 1 | 0.037223 |
| A2 | 1 | 1 | 1 | 1/4 | ½ | ½ | 1 | 1/2 | 1/2 | 1/2 | 1/4 | 1/2 | 1 | 1 | 0.037223 |
| A3 | 1 | 1 | 1 | 1/4 | ½ | ½ | 1 | 1/2 | 1/2 | 1/2 | 1/4 | 1/2 | 1 | 1 | 0.037223 |
| A4 | 4 | 4 | 4 | 1 | 2 | 3 | 4 | 3 | 3 | 2 | 1 | 3 | 4 | 4 | 0.165700 |
| A5 | 2 | 2 | 2 | 1/2 | 1 | 2 | 3 | 2 | 2 | 1 | 1/2 | 2 | 3 | 3 | 0.098906 |
| A6 | 2 | 2 | 2 | 1/3 | ½ | 1 | 2 | 1 | 1 | 1/2 | 1/3 | 1 | 2 | 2 | 0.063562 |
| A7 | 1 | 1 | 1 | 1/4 | ½ | ½ | 1 | 1/2 | 1/2 | 1/2 | 1/4 | 1/2 | 1 | 1 | 0.034956 |
| A8 | 2 | 2 | 2 | 1/3 | ½ | 1 | 2 | 1 | 1 | 1/2 | 1/3 | 1 | 2 | 2 | 0.063562 |
| A9 | 2 | 2 | 2 | 1/3 | ½ | 1 | 2 | 1 | 1 | 1/2 | 1/3 | 1 | 2 | 2 | 0.063562 |
| A10 | 2 | 2 | 2 | 1/2 | 1 | 2 | 3 | 2 | 2 | 1 | 1/2 | 2 | 3 | 3 | 0.098906 |
| A11 | 4 | 4 | 4 | 1 | 2 | 3 | 4 | 3 | 3 | 2 | 1 | 3 | 4 | 4 | 0.165700 |
| A12 | 2 | 2 | 2 | 1/3 | ½ | 1 | 2 | 1 | 1 | 1/2 | 1/3 | 1 | 2 | 2 | 0.063562 |
| A13 | 1 | 1 | 1 | 1/4 | 1/3 | ½ | 1 | 1/2 | 1/2 | 1/3 | 1/4 | 1/2 | 1 | 1 | 0.034956 |
| A14 | 1 | 1 | 1 | 1/4 | 1/3 | ½ | 1 | 1/2 | 1/2 | 1/3 | 1/4 | 1/2 | 1 | 1 | 0.034956 |

The principal Eigen value, $\lambda_{max}$ = 14.142045, CR = 0.000542

| Table 9 : Alternative matrix with respect to criteria Spot Strength (C2) | | | | | | | | | | | | | | | |
|---|---|---|---|---|---|---|---|---|---|---|---|---|---|---|---|
| C2 | A1 | A2 | A3 | A4 | A5 | A6 | A7 | A8 | A9 | A10 | A11 | A12 | A13 | A14 | Local Weight |
| A1 | 1 | 1/2 | 1/3 | 1/3 | 1/3 | 1/2 | 1/2 | 1/2 | 1/3 | 1/3 | 1/2 | 1/5 | 1/9 | 1/8 | 0.017150 |
| A2 | 2 | 1 | 1/2 | ½ | ½ | 1 | 1 | 1 | 1/2 | 1/2 | 1 | 1/4 | 1/8 | 1/7 | 0.027252 |
| A3 | 3 | 2 | 1 | 1 | 1 | 2 | 2 | 2 | 1 | 1 | 2 | 1/3 | 1/7 | 1/6 | 0.047979 |
| A4 | 3 | 2 | 1 | 1 | 1 | 2 | 2 | 2 | 1 | 1 | 2 | 1/3 | 1/7 | 1/6 | 0.047979 |
| A5 | 3 | 2 | 1 | 1 | 1 | 2 | 2 | 2 | 1 | 1 | 2 | 1/3 | 1/7 | 1/6 | 0.047979 |
| A6 | 2 | 1 | 1/2 | ½ | ½ | 1 | 1 | 1 | 1/2 | 1/2 | 1 | 1/4 | 1/8 | 1/7 | 0.027252 |
| A7 | 2 | 1 | 1/2 | ½ | ½ | 1 | 1 | 1 | 1/2 | 1/2 | 1 | 1/4 | 1/8 | 1/7 | 0.027252 |
| A8 | 2 | 1 | 1/2 | ½ | ½ | 1 | 1 | 1 | 1/2 | 1/2 | 1 | 1/4 | 1/8 | 1/7 | 0.027252 |
| A9 | 3 | 2 | 1 | 1 | 1 | 2 | 2 | 2 | 1 | 1 | 2 | 1/3 | 1/7 | 1/6 | 0.047979 |
| A10 | 3 | 2 | 1 | 1 | 1 | 2 | 2 | 2 | 1 | 1 | 2 | 1/3 | 1/7 | 1/6 | 0.047979 |
| A11 | 2 | 1 | 1/2 | ½ | ½ | 1 | 1 | 1 | 1/2 | 1/2 | 1 | 1/3 | 1/7 | 1/6 | 0.028449 |
| A12 | 5 | 4 | 3 | 3 | 3 | 4 | 4 | 4 | 3 | 3 | 3 | 1 | 1/5 | 1/4 | 0.105855 |
| A13 | 9 | 8 | 7 | 7 | 7 | 8 | 8 | 8 | 7 | 7 | 7 | 5 | 1 | 2 | 0.278896 |
| A14 | 8 | 7 | 6 | 6 | 6 | 7 | 7 | 7 | 6 | 6 | 6 | 4 | 1/2 | 1 | 0.220749 |

The principal Eigen value, $\lambda_{max}$ = 14.291379,, CR = 0.001027

| Table 10: Alternative matrix with respect to criteria Nugget Diameter (C3) | | | | | | | | | | | | | | | |
|---|---|---|---|---|---|---|---|---|---|---|---|---|---|---|---|
| C3 | A1 | A2 | A3 | A4 | A5 | A6 | A7 | A8 | A9 | A10 | A11 | A12 | A13 | A14 | Local Weight |
| A1 | 1 | 1 | 1 | 1 | ½ | 1/2 | 4 | 1 | 1/4 | 1 | ¼ | 1/2 | 1/6 | 1/6 | 0.030565 |
| A2 | 1 | 1 | 1 | 1 | ½ | 1/2 | 3 | 1 | 1/4 | 1 | 1/3 | 1/2 | 1/6 | 1/6 | 0.031992 |
| A3 | 1 | 1 | 1 | 1 | ½ | 1/2 | 3 | 1 | 1/4 | 1 | 1/3 | 1/2 | 1/6 | 1/6 | 0.031992 |
| A4 | 1 | 1 | 1 | 1 | ½ | 1/2 | 3 | 1 | 1/4 | 1 | 1/3 | 1/2 | 1/6 | 1/6 | 0.031992 |
| A5 | 2 | 2 | 2 | 2 | 1 | 1 | 6 | 2 | 1/2 | 2 | 1/3 | 1 | 1/5 | 1/5 | 0.053871 |
| A6 | 2 | 2 | 2 | 2 | 1 | 1 | 6 | 2 | 1/2 | 2 | 1/3 | 1 | 1/5 | 1/5 | 0.053871 |
| A7 | 1/4 | 1/3 | 1/3 | 1/3 | 1/6 | 1/6 | 1 | 1/4 | 1/7 | 1/4 | 1/7 | 1/6 | 1/8 | 1/8 | 0.011388 |
| A8 | 1 | 1 | 1 | 1 | ½ | 1/2 | 4 | 1 | 1/4 | 1 | ¼ | 1/2 | 1/6 | 1/6 | 0.030565 |
| A9 | 4 | 3 | 3 | 3 | 3 | 3 | 7 | 4 | 1 | 4 | 1 | 3 | 1/3 | 1/4 | 0.097385 |
| A10 | 1 | 1 | 1 | 1 | ½ | 1/2 | 4 | 1 | 1/4 | 1 | ¼ | 1/2 | 1/6 | 1/6 | 0.030565 |
| A11 | 4 | 4 | 4 | 4 | 2 | 2 | 7 | 4 | 1 | 4 | 1 | 3 | 1/3 | 1/4 | 0.111002 |
| A12 | 2 | 2 | 2 | 2 | 1 | 1 | 6 | 2 | 1/3 | 2 | 1/3 | 1 | 1/6 | 1/6 | 0.051808 |
| A13 | 6 | 6 | 6 | 6 | 5 | 5 | 8 | 6 | 3 | 6 | 3 | 6 | 1 | 1/2 | 0.199011 |
| A14 | 6 | 6 | 6 | 6 | 5 | 5 | 8 | 6 | 4 | 6 | 4 | 6 | 2 | 1 | 0.233993 |

The principal Eigen value, $\lambda_{max}$ = 14.51273, CR = 0.001922

In the criteria matrix, tensile shear strength (C2) is given the maximum weight for the reason that it is found through the destructive test confirming weld quality without any doubt. It is followed by nugget diameter, which many researchers consider a dominating factor in determining weld quality. Although the visual inspection and observation of penetration got a lower weight, compared to the other two, it is also a good factor in determining weld quality. However, surface appearance only may not necessarily confirm a good weld.

Local weights are determined following the standard method [28,29,31]. Similarly, pair-wise matrices for alternatives are constructed for each of the three criteria, and are given in Table 8, Table 9 and Table 10. Finally, global weights are determined combining the criteria matrix and alternative matrices for each criterion following the standard AHP method and shown in Table 11. It shows that the alternative A13 has the highest global weight of all the others, and hence, this parametric combination with 8 kA welding current and 5 cycle of weld time is considered to be the optimum one with the weights chosen by the authors within the experimental domain. In the used AHP algorithm, maximum weight is assigned to the tensile shear strength, this being considered to be the primary requirement, and correspondingly, the AHP gives the optimum condition that is somewhat different from the macroscopic observation of the weld nuggets. However, depending on different considerations regarding the importance of the criteria, the optimum condition would vary following the flexibility of the AHP.

**Table 11:**
Global weight of the Alternatives

| Alternatives | Weight |
|---|---|
| A1 | 0.022567 |
| A2 | 0.029416 |
| A3 | 0.042668 |
| A4 | 0.053839 |
| A5 | 0.054020 |
| A6 | 0.037695 |
| A7 | 0.023579 |
| A8 | 0.031316 |
| A9 | 0.062857 |
| A10 | 0.047640 |
| A11 | 0.062979 |
| A12 | 0.087384 |
| A13 | 0.235820 |
| A14 | 0.208220 |

## CONCLUSIONS

In this work, 17-4 PH stainless steel sheets are joined by resistance spot welding in different welding conditions. Following conclusions may be drawn from the results obtained.

- Welding parameters are optimized for 0.6 mm thick sheets at a load of 4 kN within the experimental domain. At the welding current of 2.5 kA and welding time of 6 to 7 cycles, and at the weld current of 6 to 7 kA with weld time of 5 cycles, good weld nuggets are obtained.
- At high current and time, due to excessive heat input, it results in wider HAZ and weld defects in some cases.
- The Analytical Hierarchy Process (AHP) is used for optimisation in this work. Corresponding to the requirement of maximum tensile shear strength, the AHP gives the optimum condition for resistance spot welding in the experimental domain to be at 8 kA weld current and 5 cycles of welding time within the experimental range. Depending on one's consideration regarding the importance of the criteria, the optimum condition would vary following the AHP methodology.

## REFERENCES


1. Metals Handbook (1988). Ninth Edition: Volume 6, Welding, Brazing and Soldering, 469-493.
2. Technical Data Sheet/ 17-4 Ph Stainless Steel, A K Steel Corporation, UNS S17400, www.aksteel.com.
3. Murayama M, Katayama Y and Hono K (1999). Microstructural evolution in a 17-4 PH stainless steel after aging at 400°C, Metall. Mater. Transaction A, 30A, 345-353.
4. Patrick E P, Auhl J R and Sun T S (1984). Understanding the process mechanisms is key to reliable resistance spot welding aluminum auto body components. SAE Technical Paper 840291.
5. Vural M and Akkus A (2004). On the resistance spot weldability of galvanized interstitial free steel sheets with austentic stainless steel sheets, Journal of Materials Processing Technology, 6(1), 153-154.
6. Vural M, Akkus A and Eryurek B (2006) . Effect of welding nugget diameter on the fatigue strength of the resistance spot welded joints of different steel sheets, Journal of Materials Processing Technology, 176, 127-132.
7. Kahraman N (2007). The influence of welding parameters on the joint strength of resistance spot-welded titanium sheets, Materials and Design, 28, 420-427.
8. Aslanlar S, Ogur A, Ozsarac U, Ilhan E and Demir Z (2007). Effect of welding current on mechanical properties of galvanized chromided steel sheets in electrical resistance spot welding, Materials and Design, 28, 2-7.
9. Mukhopadhyay G, Bhattacharya S and Ray K K (2009). Strength assessment of spot-welded sheets of interstitial free steels, Journal of Materials Processing Technology, 209 (4), 1995-2007.
10. Marashi P, Pouranvari M, Amirabdollahian S, Abedi A and Goodarzi M (2008). Microstructure and failure behavior of dissimilar

resistance spot welds between low carbon galvanized and austenitic stainless steels, Materials Science and Engineering, 480 (1-2), 175-180.

11. Aslanlar S, Ogur A, Ozsarac U and Ilhan E (2008). Welding time effect on mechanical properties of automotive sheets in electrical resistance spot welding, Materials and Design, 29, 1427-1431.

12. Choi B H, Joob D H and Song S H (2007). Observation and prediction of fatigue behavior of spot welded joints with triple thin steel plates under tensile-shear loading, International Journal of Fatigue, 29(4), 620-627.

13. Maa C, Chen D L, Bhole S D, Boudreau G, Lee A and Biro E (2008). Microstructure and fracture characteristics of spot-welded DP600 steel, Materials Science and Engineering: A, 485(1-2), 334-346.

14. Ahmet H and Ramazan K (2007). Resistance spot weldability of dissimilar materials (AISI 316L-DIN EN 10130-99 steels), Materials and Design, 28, 1794-1800.

15. Kocabekir B, Ramazan K, Gunduz S and Hayat F (2008). An effect of heat input, weld atmosphere and weld cooling conditions on the resistance spot weldability of 316L austenitic stainless steel, Journal of Materials Processing Technology, 195, 327-335.

16. Long X and Khanna S K (2007). Fatigue properties and failure characterization of spot welded high strength steel sheet, International Journal of Fatigue, 29, 879-886.

17. Shamsul J B and Hisyam M M (2007). Study of spot welding of austenitic stainless steel type 304, Journal of Applied Sciences Research, 3(11), 1494-1499.

18. Martin O, Tiedra P D, Lopez M, San-Juan M, Garcia C, Martin F and Blanco Y (2009). Quality prediction of resistance spot welding joints of 304 austenitic stainless steel, Materials and Design, 30(1), 68-77.

19. Qiu R, Iwamoto C and Satonaka S (2009). Interfacial microstructure and strength of steel/aluminum alloy joints welded by resistance spot welding with cover plate, Journal of Materials Processing Technology, 209(8), 4186-4193.

20. Feramuz K, Ramazan K and Gunduz S (2009). The effect of process parameter on the properties of spot welded cold deformed AISI304 grade austenitic stainless steel, Journal of Materials Processing Technology, 209(8), 4011-4019.

21. Mukhopadhyay G, Bhattacharya S and Ray K K (2009). Effect of pre-strain on the strength of spot-welds; Materials and Design, 30(7), 2345-2354.

22. Lamouroux E H J, Coutellier D, Doelle N and Kuemmerlen P (2007). Detailed model of spot welded joints to simulate the failure of car assemblies, International Journal of Interact Des Manuf., 1, 33-40.

23. Long X, Khanna S K and Allard L F (2007). Effect of fatigue loading and residual stress on microscopic deformation mechanisms in a spot welded joint, Material Science Engineering- A, 454-455, 398-406.

24. Kim D H and Kim H K (2009). Fatigue strength evaluation of cross-tension spot weld joints of cold rolled mild steel sheet, Materials and Design, 30(8), 3286-3290.

25. Aravinthan A, Sivayoganathan K, Al-Dabass D and Balendran V (2001). A neural network system for spot weld strength prediction, Proceedings of the 9th International Conference on Computer Modeling & Simulation, Cambridge, England.

26. Gupta P, Ghosh P K, Nath K and Ray S (1990). Resistance spot weldability of plain carbon and low alloy dual phase steels, Z Metallkd, 81(7), 502-508.

27. Harlin N and Jones T B (2003). Weld growth mechanism of resistance spot welds in zinc coated steels, Journal of Materials Processing Technology, 143-144, 448-453.

28. Sabiruddin K, Das S and Bhattacharya A (2009). Application of the analytic hierarchy process for optimisation of process parameters in GMAW, Indian Welding Journal, 42(1), 38-46.

29. Das S and Biswas N (2010). Process optimisation in P91 steel pipe welding, Proceedings of the National Welding Seminar- 2010, Visakhapatnam, India, 47.

30. Sarkar A and Das S (2011). Application of grey-based Taguchi method for optimising gas metal arc welding of stainless steels, Indian Welding Journal, 44(1), 37-48.

31. Saaty T L (1977). A scaling method for priorities in hierarchical structures, Journal of Mathematical Psychology, 15, 234-281.